Vol 11 No 1, January 2002
1009-1963/2002/11(01)/0072-05
Chinese Physics
© 2002 Chin. Phys. Soc.
and IOP Publishing Ltd

Phase boundary of the hexagonal-prism superconducting network in a magnetic field*

Jin Shao-Wei(金绍维), Li Wei(李 伟), Yi You-Min(易佑民),
Zhen Sheng-Lai(甄胜来), and Miao Sheng-Qing(缪胜清)
Department of Physics, Anhui University, Hefei 230039, *China*

(Received 14 March 2001; revised manuscript received 17 August 2001)

In this paper, we systematically study the phase boundary $T_c(\vec{H})$ of a hexagonal-prism superconducting network in an external magnetic field $\vec{H}$ of arbitrary magnitude and direction. The result indicates that the phase boundary of the hexagonal-prism superconducting circuit varies more sharply than that of the cubic circuit. The potential applications of the hexagonal-prism superconducting circuit are also discussed.

Keywords: superconducting network, normal-superconducting phase boundary, critical temperature
PACC: 7440, 7410

1. Introduction

It has been known for ten years that the phase boundary of superconducting networks reflects the configuration of the magnetic flux lattice on the network.[1−5] When the magnetic field is an integral number of flux quanta per unit cell, the critical temperature recovers its zero-field value, and the critical temperature $T_c(\boldsymbol{H})$ exhibits a cusp at every rational value of the flux quanta. This phenomenon corresponds to a commensurate arrangement of the vortex lattice. In the mean field approach of thin superconducting-wire networks, the critical temperature $T_c(\boldsymbol{H})$ is derived from the Ginzburg–Landau equations on each link wire, with the conservation of the current at the nodes of the lattice.[1] The critical temperature $T_c(\boldsymbol{H})$ of micrometre-sized two-dimensional (2D) hexagonal superconducting networks in an external magnetic field had been studied previously.[6,7]

In this paper we systematically study the phase boundary of a hexagonal-prism superconducting network made up of 31 identical straight thin wires, in an applied magnetic field of arbitrary magnitudes and directions. The single cubic superconducting circuit[8] made up of twelve identical wires and the multi-cube circuit[9] made up of 6×6×6 cubes have been studied previously. Comparing a hexagonal-prism superconducting circuit with a single cube circuit, one finds that the phase boundary of the hexagonal-prism circuit changes more sensitively than that of a single cube circuit. This is because the flux threading through the holes of the hexagonal-prism superconducting circuit is greater than that of a single cube circuit in an external magnetic field.

It has been shown[8,9] that the critical temperature depends in a complex and sensitive way on both the magnitude and the direction of the magnetic field. The sensitive directional dependence may have practical applications as the basis of a micrometre-sized instrument, which can either determine sensitively the orientation of this kind of instrument, or detect the magnitude and direction of a weak external magnetic field. In this paper, it will be shown that it is better to use a hexagonal-prism superconducting circuit to improve the sensitivity of the device than to use a cubic circuit.

2. Equation for the transition temperature in a hexagonal-prism superconducting network

The superconducting transition temperature for a network of thin superconducting wires in an arbitrary magnetic field can be determined by the linearized Ginzburg–Landau equations. After enforcing a certain set of boundary conditions first derived by de Gennes,[1] at the nodes of the network, one then obtains a set of equations which govern the values of the order parameter at the nodes, and has a generalized eigenvalue problem. When all of the strands have the same cross-sectional area and physical characteristics, the equation corresponding to node α is given

*Project supported by the Education Foundation of Anhui Province, China (Grant Nos. 1997JL099 and 2000JL006).

by[2–5]

$$\sum_{\beta=1}^{n}[-\psi_\alpha \cot(L_{\alpha\beta}/\xi)+\psi_\beta \exp(-\mathrm{i}\gamma_{\alpha\beta})/\sin(L_{\alpha\beta}/\xi)]=0, \quad (1)$$

where ψ_α is the value of the (complex) superconducting order parameter at the αth node of the network, $L_{\alpha\beta}$ is the length of the strand connecting the node α with the node β, and $\xi(T)=\xi(0)(1-T/T_{c0})^{-1/2}$ is the coherence length. T_{c0} is the zero-field transition temperature of the superconducting material used, and also the transition temperature of the network at no applied field. $\gamma_{\alpha\beta} \equiv (2\pi/\Phi_0)\int_\alpha^\beta \boldsymbol{A}\cdot \mathrm{d}l$ is the phase factor which is due to the external field and the vector potential $\boldsymbol{A}$, and the flux quantum $\Phi_0(\equiv hc/2e)$, the integral being along the strand connecting the nodes α and β. The summation "$\sum_{\beta=1}^{n}$" runs over all nodes β which are linked to node α. Clearly, one has as many equations as the number of nodes in the network, which are solved as coupled equations. The temperature may be considered as the generalized eigenvalue of this set of equations, and the transition temperature $T_c(\boldsymbol{H})$ should be identified as the largest among all such generalized eigenvalues. Note that the highest $T_c(\boldsymbol{H})$ also corresponds to the largest $\lambda=\cos[L/\xi(T)]$. In this paper we consider a network of a hexagonal-prism lattices (see Fig.1). In the present problem all the network links are of equal length (i.e. all $L_{\alpha\beta}=a$). There are fourteen equations corresponding to the fourteen nodes which may be combined into a single matrix equation as

$$\begin{bmatrix} m_{1,1} & m_{1,2} & \cdots & m_{1,14} \\ m_{2,1} & m_{2,2} & \cdots & m_{2,14} \\ \vdots & \vdots & \ddots & \vdots \\ m_{14,1} & m_{14,2} & \cdots & m_{14,14} \end{bmatrix} \cdot \begin{bmatrix} \psi_1 \\ \psi_2 \\ \vdots \\ \psi_{14} \end{bmatrix} = 0, \quad (2)$$

where the diagonal matrix elements $m_{j,j}=-Z_{j,j}\lambda$ ($j=1,2,\cdots,14$), the parameter $Z_{j,j}$ is equal to 7 (j=1,8), the rest parameters $Z_{j,j}$ are all equal to 4 and $\lambda \equiv \cos[a/\xi(T)]$. The off-diagonal matrix element $m_{j,k}(j\neq k)$ is nonzero only if the node j and node k are nearest neighbours. The precise values of the nonvanishing off-diagonal matrix elements are dependent on the gauge chosen to represent the external magnetic field. The magnetic field is in an arbitrary direction relative to the network (see Fig.1). So we can write $\boldsymbol{H}=H(n_x\hat{\boldsymbol{e}}_x+n_y\hat{\boldsymbol{e}}_y+n_z\hat{\boldsymbol{e}}_z)$, where $n_x=\sin\theta\cos\varphi$, $n_y=\sin\theta\sin\varphi$ and $n_z=\cos\theta$ are the directional cosines, and (θ,φ) is a polar representation of the direction of the magnetic field vector. The gauge we have chosen is such that the vector potential $\boldsymbol{A}$ has components $A_x=Hzn_y$, $A_y=H(xn_z-zn_x)$, and A_z=0. Accordingly, the nonvanishing off-diagonal matrix element satisfies $m_{j,k(j\neq k)}=m^*_{k,j}$, and we are only left to calculate the nonvanishing matrix elements $m_{j,k}(j<k; j=1,14; k=j+1,14)$ and the matrix elements $m_{j,k}(j>k;\ k$=1,14; $j=k+1,14)=m^*_{k,j}$. The partial nonvanishing matrix elements are: $m_{1,2}=\exp(\mathrm{i}\gamma n_z)$, $m_{1,3}=\exp(-\mathrm{i}\gamma n_z)$, $m_{1,4}=1, m_{1,5}=\exp(\mathrm{i}\gamma n_z)$, $m_{1,6}=\exp(-\mathrm{i}\gamma n_z)$, $m_{1,7}=1, m_{1,8}=1$; $m_{2,3}=\exp(-4\mathrm{i}\gamma n_z)$, $m_{2,7}=\exp(\mathrm{i}\gamma n_z)$, $m_{2,9}=1$; $m_{3,4}=\exp(-\mathrm{i}\gamma n_z)$, $m_{3,10}=1$; $m_{4,5}=\exp(-\mathrm{i}\gamma n_z)$, $m_{4,11}=1$; $m_{5,6}=\exp(-4\mathrm{i}\gamma n_z)$, $m_{5,12}=1$; $m_{6,7}=\exp(-\mathrm{i}\gamma n_z)$, $m_{6,13}=1$; $m_{7,14}=1;\cdots; m_{12,13}=\exp(-\mathrm{i}(8\gamma n_x/\sqrt{3}+4\gamma n_z))$; $m_{13,14}=\exp(-\mathrm{i}(4\gamma n_y+4\gamma n_x/\sqrt{3}+\gamma n_z))$; where $\gamma=\pi\Phi/\Phi_0$, $\Phi=\sqrt{3}Ha^2/4$, and $\Phi_0\equiv hc/2e$ is the flux quantum.

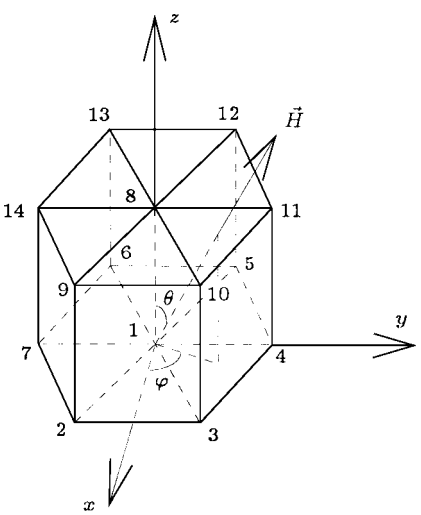


Fig.1. The coordinate system used and the definition of a hexagonal-prism circuit.

To calculate the field-dependent transition temperature $T_c(\boldsymbol{H})$ of the network, by setting the determinant of the above matrix $\boldsymbol{M}$ equal to zero (i.e. det$\boldsymbol{M}$=0), we obtain a polynomial equation of fourteenth degree on λ, and by solving the polynomial equation we obtain the fourteen roots λ_s (s=1,2,$\cdots$,14). These fourteen roots give fourteen positive values for $(a/\xi)^2$, the smallest $(a/\xi)^2$ determines the $T_c(\boldsymbol{H})$ of the network. Since $\xi(T)=\xi(0)(1-T/T_{c0})^{-1/2}$, the smallest $(a/\xi)^2$ is directly proportional to the per cent reduction of the transition temperature $(1-T/T_{c0})$. (Note that Eq.(2) has the form $(\boldsymbol{M}'-\lambda\boldsymbol{E})\Psi$=0, where $\boldsymbol{M}'$ has only the

off-diagonal matrix elements of $\boldsymbol{M}$, whereas $\boldsymbol{E}$ is a diagonal matrix, but not an identity matrix. Thus Eq.(2) is a generalized eigenvalue equation.) The approach to solving the polynomial equation needs much computing time. In this paper, the phase boundary is obtained by directly solving the matrix equation eigenvalue (for details of this approach see Ref.[6]), so that the computing time is greatly reduced, and the result is same as that of solving the polynomial equation.

3. Numerical result

The results of Eq.(2) are shown in the following seven figures. In Figs.2–4, the θ dependence of $(a/\xi)^2$ is plotted for three values of φ, namely 0°, 14.04° ($\tan^{-1}(1/4)$) and 30°, and each for three values of Φ/Φ_0, namely 0.25, 0.50 and 0.75. Figures 5–7 are extensions of Figs.2–4, respectively, to three larger values of Φ/Φ_0, namely 1.0, 2.0 and 5.0. (Here, we do not need to calculate beyond 90° in θ, and 30° in φ, for the network has a hexagonal-prism symmetry. Figure 1 may help readers to see this point easily.) From Figs.2–7, it can be seen that the dependence of the transition temperature on the two angles θ and φ becomes more sensitive and complicated, as Φ/Φ_0 is increased to a larger value beyond unity (Φ/Φ_0=1), so that even with three figures at three roughly equally spaced values of φ, it is not difficult to visualize the continuous variation of the transition temperature with the angle φ. On the other hand, for $\Phi/\Phi_0 < 1$, this dependence is much less complicated, so one does not really need three figures (Figs.2–4) to see this continuous variation, although these figures are given in this paper.

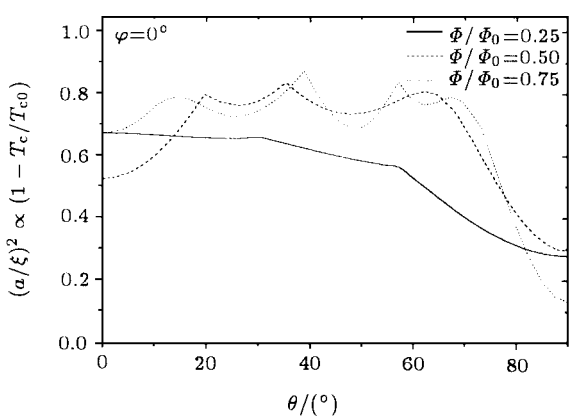


Fig.2. Plot of $(a/\xi)^2 \propto (1-T_c/T_{c0})$ as a function of θ for φ=0 and for three values of Φ/Φ_0: 0.25, 0.50 and 0.75.

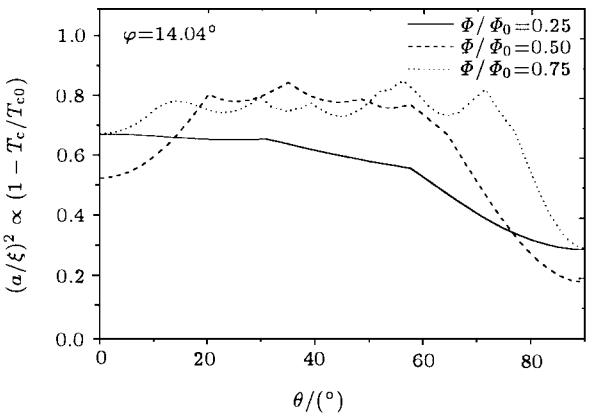


Fig.3. Same as Fig.2 except that $\varphi=\tan^{-1}(1/4)=14.04°$.

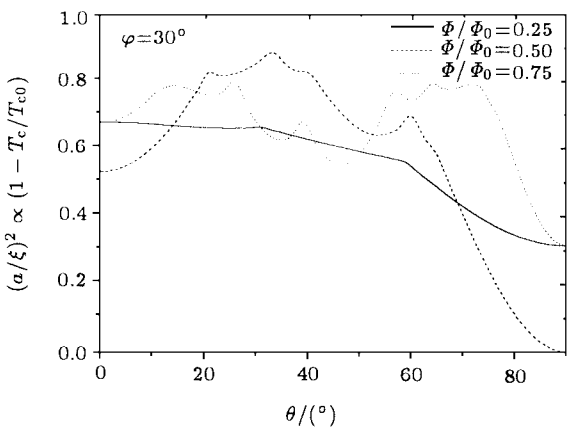


Fig.4. Same as Fig.2 except that φ=30°.

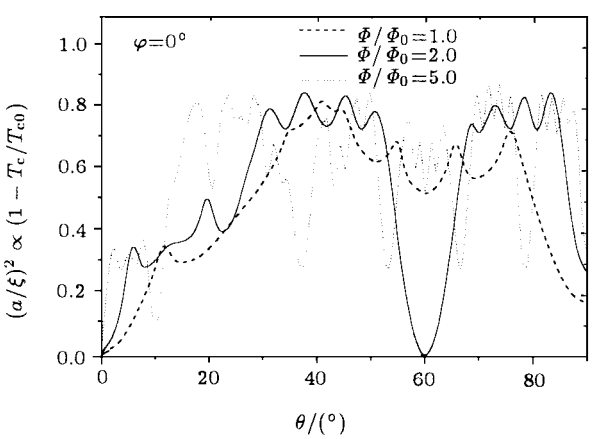


Fig.5. Same as Fig.2 except that it is now for three new values of Φ/Φ_0: 1.0, 2.0 and 5.0. One may combine this figure with Fig.2 to visualize to some extent how the curve $(a/\xi)^2$ versus θ changes with Φ/Φ_0 at φ=0°.

We can also see how the curve T_c versus θ evolves as Φ/Φ_0 is increased by combining Fig.2 with Fig.5, Fig.3 with Fig.6, etc. See Fig.8 for more details about this Φ/Φ_0 dependence. In Fig.8 we have plotted $(a/\xi)^2$ as a function of Φ/Φ_0 for the polar angles of $\boldsymbol{H}$

fixed at $\theta = \cos^{-1}(4/13)$, and $\varphi = \tan^{-1}(1/4)$, given directional cosines n_x=12/13, n_y=3/13, and n_z=4/13, which are all in rational ratios. For this choice, $(a/\xi)^2 \propto (1 - T_c/T_{c0})$ should drop to zero (i.e. T_c can rise to T_{c0}), whenever Φ/Φ_0 is equal to a multiple of 13—the common denominator of the directional cosines. In fact, when Φ/Φ_0 is equal to a multiple of 13.10 (or 3.277), T_c approaches T_{c0}, but cannot rise to T_{c0}. This is because the flux components through all the principal directions of a hexagonal-prism circuit are not equal to each other; this is demonstrated in Fig.8.

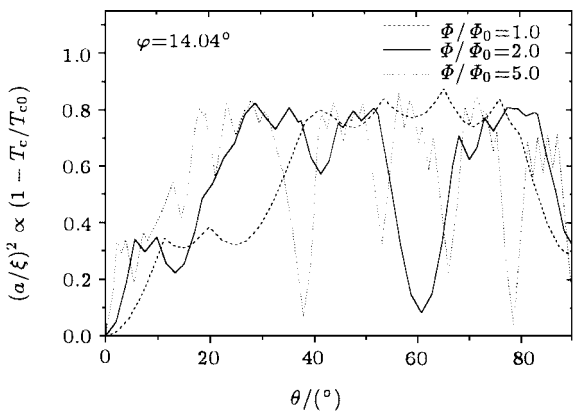


Fig.6. Same as Fig.5 except that φ=$\tan^{-1}(1/4)$=14.04° as in Fig.3. One may combine this figure with Fig.3 to visualize to some extent how the curve $(a/\xi)^2$ versus θ changes with Φ/Φ_0 at φ=14.04°.

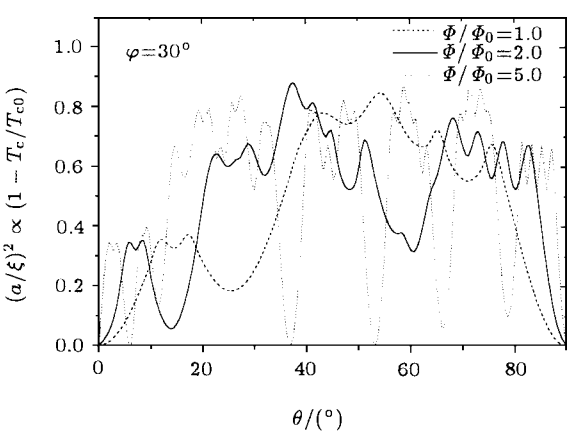


Fig.7. Same as Fig.5 except that φ=30° as in Fig.4. One may combine this figure with Fig.4 to visualize to some extent how the curve $(a/\xi)^2$ versus θ changes with Φ/Φ_0 at φ=30°.

In order to reveal the qualitative change and the general trend of the minor maxima and minima in this curve, we need to refer to the next two plots: Figs.9 and 10. In these two figures we concentrate on the vicinity of one isolated major peak of T_c/T_{c0} (i.e. one major minimum in $(a/\xi)^2 \propto (1 - T_c/T_{c0})$), and study it in detail. We study only the vicinity of the peak corresponding to Φ/Φ_0=13.10, $\theta = \cos^{-1}(4/13.10) \approx 72.22°$ and $\varphi = \tan^{-1}(1/4) \approx 14.04°$. Here, we present two 2D cross-sectional plots rather than a three-dimensional (3D) plot, in order to reveal quantitative details. In Fig.9, we keep $\varphi = \tan^{-1}(1/4)$, and plot $(a/\xi)^2$ against θ in a range of 10° covering the point $\theta = \cos^{-1}(4/13.10)$. However, in Fig.10, θ is kept at $\cos^{-1}(4/13.10)$, and we plot $(a/\xi)^2$ against φ in a range of 10° covering $\varphi = \tan^{-1}(1/4)$. Figures 9 and 10 reveal the detailed behaviour of a single major 3D peak of $T_c(\theta, \varphi)$ (shown as a major minimum of $(a/\xi)^2 \propto (1 - T_c/T_{c0})$).

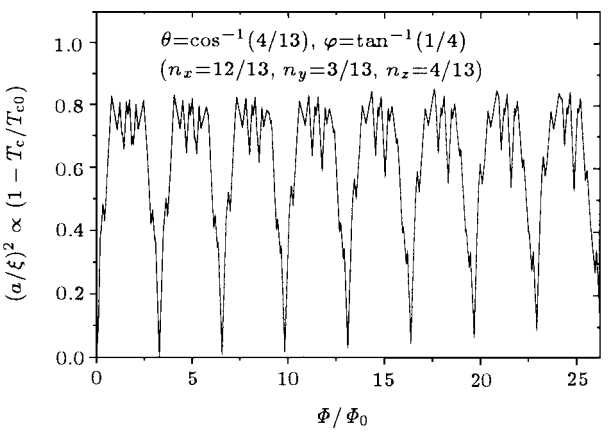


Fig.8. The plot of $(a/\xi)^2 \propto (1 - T_c/T_{c0})$ as a function of Φ/Φ_0 for the special choice of the polar θ and φ as given, in which the directional cosines of the applied magnetic field are in the rational ratios 12:3:4. This curve should be compared with Fig.12 of Ref.[8].

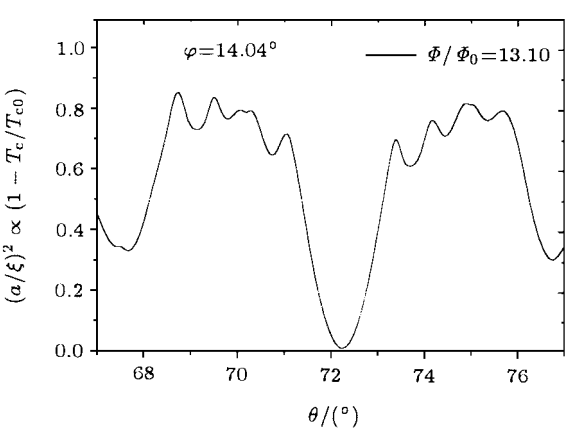


Fig.9. The plot of $(a/\xi)^2 \propto (1 - T_c/T_{c0})$ for a hexagonal-prism superconducting circuit, as a function of θ in a 10° range covering the point $\theta = \cos^{-1}(4/13.10) \approx 72.22°$, for fixed values of $\varphi = \tan^{-1}(1/4) \propto 14.04°$ and Φ/Φ_0=13.10. Important details about this figure are also given in Fig.10.

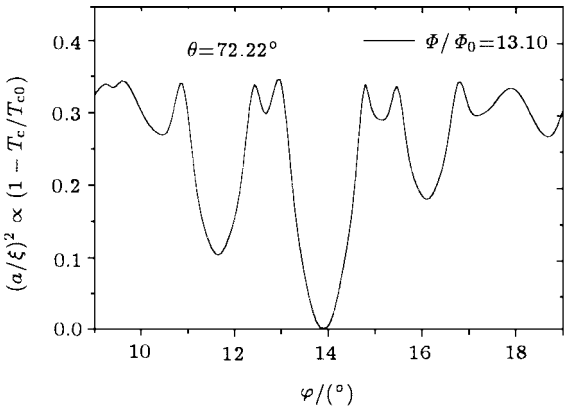


Fig.10. Same as Fig.9 except that θ is fixed at $\cos^{-1}(4/13.10) \approx 72.22°$, and φ is varied through a range of 10° covering the point $\varphi = \tan^{-1}(1/4) \approx 14.04°$. Figures 9 and 10 provide two cut-out views of a 3D profile of a major peak of $T_c(\vec{H})$ as a function of two polar angles θ and φ, describing the direction of the magnetic field $\vec{H}$ held at one of the special values for which a major peak of T_c can be obtained at certain values of θ and φ.

4. Conclusion and discussion

Comparing Figs.6 and 7 of Ref.[9] with Figs.9 and 10 in this paper, we have found that the major peak of T_c/T_{c0} of the hexagonal-prism circuit is much sharper than that of a cubic circuit. This change in the qualitative behaviour of the major peak of $T_c(\boldsymbol{H})$ has been already reported in Ref.[6] based on knowledge of hexagonal circuits, and it is explicitly confirmed in this paper. This confirmation is so important that any applications of such circuits will probably rely on the behaviour of their $T_c(\boldsymbol{H})$ near one of these major peaks (see Ref.[8]). This means that the value of $T_c(\boldsymbol{H})$ will deviate from T_c with the variation of the magnitude and direction of the external magnetic field vector. Here, set T_c is equal to $T_c(\boldsymbol{H})$ of the major peak climax.

In summary, we have presented an exact calculation of the phase boundary of a hexagonal-prism superconducting circuit made of 31 identical straight thin wires in an external magnetic field of arbitrary magnitude and direction. We have extended the previous calculation of the phase boundary $T_c(\boldsymbol{H})$ of single-cube and multi-cube superconducting circuits to a hexagonal-prism circuit. We obtain the result that the T_{c0} drops sharply to $T_c(\boldsymbol{H})$ (see Figs.9 and 10). This phenomenon clearly shows that the feedback circuit made up of a hexagonal-prism circuit is superior to that of a cubic circuit in controlling the orientation of a device and determining an unknown feeble external magnetic field. The device containing a multi-hexagonal-prism network is more sensitive than that containing a single hexagonal prism. However, the fabrication of a multi-hexagonal-prism network is probably still a challenge to the present-day laser-carving technology. It is helpful that experimentalists start by trying to carve a hexagonal-prism circuit to let us compare the experimental results with the calculated results. We expect that the study of a single hexagonal-prism circuit is beneficial to further research on multi-hexagonal-prism circuits.

References

[1] De Gennes P G 1981 *C. R. Acad. Sci., Paris* **292** 279

[2] Alexander S 1983 *Phys. Rev.* B **27** 1541

[3] Rammal R, Lubensky T G and Toulouse G 1983 *Phys. Rev.* B **27** 2820

[4] Fink H J, Lopez A and Maynard R 1982 *Phys. Rev.* B **26** 5237

[5] Simonin J, Rodrigues D and Lopez A 1982 *Phys. Rev. Lett.* **49** 944

[6] Jin S W, Miao S Q and Yi Y M 1999 *J. Low Temp. Phys.* **21** 143 (in Chinese)

[7] Jin S W *et al* 1999 *J. Anhui University (Nat.)* **23** 21 (in Chinese)

[8] Hu C R and Huang C H 1991 *Phys. Rev.* B **43** 7718

[9] Yi Y M and Hu C R 1992 *Phys. Rev.* B **46** 5448